Study of Kuo-Type Cumulus Parameterizations during Different Epochs of the Asian Summer Monsoon

SOMESHWAR DAS, U. C. MOHANTY AND O. P. SHARMA

Centre for Atmospheric Sciences, Indian Institute of Technology, Hauz Khas, New Delhi, India

(Manuscript received 22 December 1986, in final form 23 September 1987)

ABSTRACT

The performances of several versions of the Kuo-type cumulus parameterization schemes have been examined during different phases of the summer monsoon. These phases are the preonset, an onset and a period of break in the monsoon. Special sets of upper air observations that were collected from stationary ships forming polygons over the Arabian Sea and the Bay of Bengal during MONEX-79 were used for this purpose. Cumulus warming, drying and precipitation rates have been simulated in a semiprognostic way and compared with the observations.

The limitations of different schemes for numerical weather prediction are discussed. Among various Kuo-type cumulus parameterization schemes studied in this article, a modified Kuo-scheme is found to provide best results during the summer monsoon. In this scheme the moistening parameter is determined based upon the relative humidity and it is tuned for different phases of the monsoon.

A comparison of the performance of various schemes during different phases of the monsoon was made. The heating and drying rates were best simulated during a preonset phase, when compared with the other two periods. The largest deviations between observed and simulated values were obtained during a break in the monsoon.

1. Introduction

Perhaps the most widely used scheme to parameterize cumulus convection in large scale numerical weather prediction is that proposed by Kuo (1965, 1974). After its inception in 1965, the scheme has undergone several modifications, including the one made by Kuo himself in 1974, where he emphasized the need for a moistening parameter. The necessity of such a parameter was felt because Kuo's earlier scheme underestimated rainfall and cumulus heating. Anthes (1977) proposed that the moistening parameter '*b*' be computed from the relative humidity of the environment. Krishnamurti et al. (1983b, hereafter referred to as KLP) proposed an ultimate-Kuo scheme that prescribed an upper limit to the vertical structure of heating and moistening attainable by the Kuo's scheme. They also emphasized the need for a mesoscale convergence parameter and obtained a closure of this scheme by a multiple regression approach. Molinari (1985) generalized the Kuo's scheme to satisfy arbitrary vertical profiles of apparent heat source and moisture sink. All these versions of the Kuo's scheme are now referred to as Kuo-type cumulus parameterization schemes.

The simplicity and efficiency of Kuo's scheme and its economy in computer time has made it convenient for numerical weather prediction. But, it is desirable to examine its performance in the light of reality. One way to do it is to use the parameterization scheme in a semiprognostic way (one time step forecast), so that the results are free from other modelling errors. With this view in mind, we have applied different versions of the Kuo-type cumulus parameterization schemes to the special observations that were collected from ships over the Arabian Sea and the Bay of Bengal during the Monsoon Experiment of 1979 (MONEX-79). These datasets cover a wide range of situations involving different degrees of convective activity during three epochs of the Asian summer monsoon. These phases refer to (a) preonset, (b) onset and (c) a period of break in the monsoon.

Section 2 describes different versions of the Kuo-type cumulus parameterization schemes. Section 3 describes the datasets used in this study. The results are presented in section 4 and, finally, the conclusions are summarized in section 5.

2. Kuo-type cumulus parameterizations

a. Broad features

The purpose of this paper is to evaluate different modifications of Kuo's cumulus parameterization technique, with computations based on data collected during the Monsoon Experiment (MONEX) of 1979. The different versions are summarized in Table 1.

For clarity and continuity, we present a short resume

Corresponding author address: Dr. U. C. Mohanty, Centre for Atmospheric Sciences, Indian Institute of Technology, Hauz Khas, New Delhi-110016, India.

TABLE 1. Summary of different versions of Kuo's scheme.

Scheme	Authors	Principal features
K65	Kuo (1965)	Computes convergence of moisture and rate of cloud production.
K74	Kuo (1974)	Introduces moistening parameter to separate moistening from rain production.
K-AN I	Anthes (1977)	Moistening parameter defined by critical relative humidity.
K-AN II	Kuo and Anthes (1984)	Introduces adjustment tune for rain production.
K-REG	Krishnamurti et al. (1983b)	Large scale heating and moistening determined by regression equations.
K-UL	Krishnamurti et al. (1983b)	Prescribes an upper limit to the vertical structure of heating and drying attainable by a Kuo-type scheme.
K-MO	Molinari (1985)	Satisfies arbitrary vertical profiles of heating and drying based on specified apparent heat source and moisture sink.

of the details of each scheme mentioned in the Table 1. In Kuo's scheme, the cumulus heating and drying are invoked when (i) the atmosphere is conditionally unstable, i.e.

$$-\left(\frac{T}{\theta}\frac{\partial\theta}{\partial p}+\frac{L}{C_p}\frac{\partial q}{\partial p}\right)<0 \tag{1}$$

and (ii) there is a net convergence of moisture over the grid scale given by

$$I_L=-\frac{1}{g}\int_{P_t}^{P_b}\omega\frac{\partial q}{\partial p}\,dp>0 \tag{2}$$

The different symbols are explained in Table 2. In this study, the cloud base was taken to be at the lowest unstable layer for which the relative humidity exceeded a critical value, chosen as 0.8 (Molinari, 1982). The temperatures inside the cloud are then calculated by following the local moist adiabat from the cloud base.

The total moisture supply I is defined as the sum of the large-scale moisture supply I_L and a nonmeasurable mesoscale moisture supply $I_L\eta$ i.e.,

$$I=I_L(1+\eta) \tag{3}$$

where η is a mesoscale convergence parameter.

A part of the moisture condenses and precipitates out while the remaining part moistens the atmosphere. Thus, the total moisture supply is partitioned as

$$I=R+M \tag{4a}$$

$$=I(1-b)+Ib \tag{4b}$$

$$=I_\theta+I_q \tag{4c}$$

$$\text{where } I_\theta=a_\theta Q_\theta \quad\text{and}\quad I_q=a_qQ_q. \tag{4d}$$

The total supply of moisture Q required to form a cloud on a grid scale is given by

$$Q=Q_q+Q_\theta \tag{5a}$$

where

$$Q_q=\frac{1}{g}\int_{p_t}^{p_B}\frac{q_c-q}{\Delta\tau}\,dp \tag{5b}$$

$$Q_\theta=\frac{1}{g}\int_{p_t}^{p_B}\left[\frac{C_PT(\theta_c-\theta)}{L\theta\Delta\tau}+\omega\frac{C_P}{L}\frac{T}{\theta}\frac{\partial\theta}{\partial p}\right]dp. \tag{5c}$$

Here Q_q denotes the supply of moisture required to change the environmental humidity from q to a local moist adiabat q_c in time scale $\Delta\tau$. The $\Delta\tau$ is taken to be 20 minutes. Molinari (1982) has shown that $\Delta\tau$ does not play role in the vertical mean temperature and

TABLE 2. List of symbols.

Symbol	Description
a_1, b_1, c_1	Coefficients of multiple regression for moistening
a_2, b_2, c_2	Coefficients of multiple regression for rainfall
a_θ, a_q	Constants of proportionality for heating and moistening by clouds
b	Moistening parameter
c	Condensation rate
C_P	Specific heat of air at constant pressure
e	Evaporation rate
g	Acceleration due to gravity
I, I_L	Total moisture supply and the large scale moisture supply
I_q, I_θ	Part of moisture stored in the atmosphere and that condensed as precipitation
L	Latent heat of condensation
M	Moistening rate
p, p_b, p_t	Pressure, cloud base pressure and cloud top pressure
Q	Total supply of moisture required to form cloud
Q_1, Q_2	Apparent heat source and moisture sink
Q_R	Radiative heating rate
Q_q	Rate of moisture supply required to saturate the column at cloud temperature
Q_θ	Rate of moisture supply required to raise temperature at cloud temperature
q	Specific humidity
R	Rate of rainfall
RH, RH_c	Relative humidity and critical relative humidity
S	Dry static energy
T	Temperature
t	time
V	Horizontal wind speed
δ	Divergence
ξ	Relative vorticity
ω	Vertical velocity ($=dp/dt$)
$\omega'S'$	Vertical eddy flux of heat
$\omega'q'$	Vertical eddy flux of moisture
$\Delta\tau$	Cloud formation time scale (=20 min.)
θ	Potential temperature
χ_1, χ_2	Meteorological variables used in multiple regression
η	Mesoscale convergence parameter
$(\ )_c$	Cloud variable

moisture variation. The first term on the right hand side of Q_θ denotes the time required to establish a moist adiabat and the second term denotes the moisture supply required to overcome the adiabatic cooling due to large scale ascent.

The heating and moistening by the clouds is proportional to the temperature and humidity difference between the model cloud and the environment. Consequently, the conservation of entropy and moisture is expressed by

$$\frac{\partial\theta}{\partial t} + \mathbf{V}\cdot\nabla\theta + \omega\frac{\partial\theta}{\partial p} = a_\theta\left(\frac{\theta_c - \theta}{\Delta\tau} + \omega\frac{\partial\theta}{\partial p}\right) + Q_R \quad (6)$$

$$\frac{\partial q}{\partial t} + \mathbf{V}\cdot\nabla q = a_q\left(\frac{q_c - q}{\Delta\tau}\right). \quad (7)$$

The apparent heat source and moisture sink in Kuo's scheme are thus given by

$$(Q_1)_K = a_\theta\left[C_P\frac{T}{\theta}\frac{\theta_c - \theta}{\Delta\tau} + \omega C_P\frac{T}{\theta}\frac{\partial\theta}{\partial p}\right] \quad (8)$$

$$(Q_2)_K = -L\left[a_q\frac{q_c - q}{\Delta\tau} + \omega\frac{\partial q}{\partial p}\right]. \quad (9)$$

The observed apparent heat source and moisture sink are

$$Q_1 = \pi\left(\frac{\partial\bar{\theta}}{\partial t} + \bar{\mathbf{V}}\cdot\nabla\bar{\theta} + \bar{\omega}\frac{\partial\bar{\theta}}{\partial p}\right)$$

$$= Q_R + L(\bar{c} - \bar{e}) - \pi\frac{\overline{\partial\omega'\theta'}}{\partial p} \quad (10)$$

$$Q_2 = -L\left(\frac{\partial\bar{q}}{\partial t} + \bar{\mathbf{V}}\cdot\nabla\bar{q} + \bar{\omega}\frac{\partial\bar{q}}{\partial p}\right)$$

$$= L(\bar{c} - \bar{e}) + \frac{\overline{\partial\omega'q'}}{\partial p} \quad (11)$$

In Eq. (10), $\pi = C_P(p/p_0)^{R/C_P}$. In the context of this brief summary, the main features of the different schemes are explained in the following sections.

b. Kuo (1965) scheme (K65)

The expressions for a_θ and a_q in this scheme are

$$a_\theta = a_q = I_L/(Q_\theta + Q_q). \quad (12)$$

c. Kuo (1974) scheme (K74)

In this scheme, a vanishingly small value of the moistening parameter b (≈ 0) has been found to provide the best estimate of rainfall. The coefficients a_θ and a_q are defined by

$$a_\theta = I_L/Q_\theta \quad (13a)$$

$$a_q = 0. \quad (13b)$$

d. Kuo–Anthes scheme (K–AN)

Anthes (1977) defined the partitioning factor b as

$$b = \begin{cases} \left(\dfrac{1 - \langle\mathrm{RH}\rangle}{1 - \mathrm{RH}_c}\right)^n, & \langle\mathrm{RH}\rangle \geq \mathrm{RH}_c \\ 1, & \langle\mathrm{RH}\rangle \leq \mathrm{RH}_c \end{cases} \quad (14)$$

where $\langle\mathrm{RH}\rangle$ denotes a mean relative humidity in the column. RH_c is a critical relative humidity suggested to be 0.5 by Anthes and $n = 1$. As it will be shown later, this scheme provided the best results when n was between 3 and 5, and RH_c was between 0 and 0.25. In the following discussions, K-AN I denotes the unadjusted Anthes scheme while, K-AN II denotes the one after adjustment with MONEX datasets.

The coefficients a_θ and a_q are determined as

$$a_\theta = \frac{(1 - b)I_L}{Q_\theta} \quad (15a)$$

$$a_q = \frac{bI_L}{Q_q}. \quad (15b)$$

The above method is not strictly the same as that proposed by Anthes (1977). In the original scheme of Anthes, one dimensional cloud model was used to calculate the net condensation rates inside clouds. However, the parameter 'b' was the same as given by (14). Here we calculate b by the method proposed by Anthes. The heating and moistening rates are calculated using the coefficients (15a), (15b), so that the results may be readily compared with other versions of Kuo's scheme.

e. Kuo-regression approach (K-REG)

This approach was suggested by Krishnamurti et al. (1983b). The large-scale heating and moistening are expressed by the regression equations

$$\frac{M}{I_L} = (1 + \eta)b = a_1\chi_1 + b_1\chi_2 + C_1 \quad (16a)$$

$$\frac{R}{I_L} = (1 + \eta)(1 - b) = a_2\chi_1 + b_2\chi_2 + C_2 \quad (16b)$$

where χ_1 and χ_2 are any variables such as the relative vorticity ξ or the divergence δ. The a_i, b_i, c_i ($i = 1, 2$) are coefficients of regression. In the study of KLP it was found that the relative vorticity ξ at 700 mb and the vertically averaged large-scale vertical velocity $\bar{\omega}$ provided the best estimates of heating and moistening over GATE. Thus Krishnamurti et al. (1983b) chose $\chi_1 = \xi_{700}$ and $\chi_2 = \bar{\omega}$. However, we found that the horizontal divergence δ provided relatively better correlation than ξ in the present study. For three cases, the divergence at 950 mb provided relatively better correlation during the preonset and onset periods, while the divergence at 900 mb showed higher correlation during a break in the monsoon. The regression coef-

ficients a_i, b_i, c_i obtained from different studies are shown in Table 3. In (16), the ratio M/I_L was calculated by the method suggested by KLP and the ratio R/I_L was calculated using the precipitation rates estimated from the observed moisture budget. The rainfall rates measured by raingauges on ships could not be used for this purpose, because they did not represent the areal rainfall over the ship polygon.

The precipitation rate from the observed moisture budget is

$$P_{Q_2} = \frac{1}{g}\int_{100}^{p_s} \frac{Q_2}{L}\, dp + E_s \tag{17}$$

where p_s is the surface pressure and E_s is the rate of evaporation from the surface. The E_s was calculated by a bulk aerodynamic method (Thompson et al., 1979). Evaporation rates were found to be of the order of 5–10 mm day^{-1}.

From the relations (16a) and (16b), the expressions for b and η are obtained as

$$b = \frac{a_1\chi_1 + b_1\chi_2 + c_1}{(a_1 + a_2)\chi_1 + (b_1 + b_2)\chi_2 + (c_1 + c_2)} \tag{18a}$$

$$\eta = (a_1 + a_2)\chi_1 + (b_1 + b_2)\chi_2 + (c_1 + c_2) - 1. \tag{18b}$$

The coefficients a_θ and a_q are then obtained by

$$a_\theta = I_L(1 + \eta)(1 - b)/Q_\theta \tag{19a}$$

$$a_q = I_L(1 + \eta)b/Q_q. \tag{19b}$$

f. Ultimate Kuo scheme (K-UL)

The exact values of coefficients a_θ and a_q may be determined diagnostically from observations. They are expressed as

$$a_\theta = \frac{\bar{Q}_1(p_B - p_t)/g}{Q_\theta} \tag{20a}$$

$$a_q = \frac{-\left\{\dfrac{\bar{Q}_2}{L}\dfrac{(p_B - p_t)}{g} - I_L\right\}}{Q_q} \tag{20b}$$

where $\bar{Q}_1$ and $\bar{Q}_2$ are the column averaged observed apparent heat source and moisture sink.

The exact or observed estimates of b and η are given by

$$b = \frac{a_qQ_q}{a_\theta Q_\theta + a_qQ_q} \tag{21a}$$

$$\eta = \frac{a_\theta Q_\theta + a_qQ_q}{I_L} - 1. \tag{21b}$$

g. Kuo–Molinari scheme (K-MO)

Molinari (1985) proposed a method where the apparent heat source $(Q_1)_K$ and moisture sink $(Q_2)_K$ from the Kuo's scheme satisfy an arbitrary distribution of Q_1 and Q_2. In this approach, the equations for $(Q_1)_K$ and $(Q_2)_K$ are given by

$$(Q_1)_K = gL(1 - b)\frac{I_L\alpha}{\displaystyle\int_{p_t}^{p_b} \alpha dp} \tag{22a}$$

$$(Q_2)_K = -L\left(gbI_L\frac{\beta}{\displaystyle\int_{p_t}^{p_b}\beta dp}\omega\frac{\partial\bar{q}}{\partial p}\right) \tag{22b}$$

where

$$b = \frac{J + I_L}{I_L}\left(\frac{Q_q}{Q_q + Q_\theta + J}\right) \tag{23}$$

$$J = -\frac{1}{g}\int_{p_t}^{p_b}\frac{C_pT}{L}\omega\frac{\partial\theta}{\partial p}\, dp$$

$$\alpha = Q_1 \tag{24a}$$

$$\frac{\beta}{\displaystyle\int_{p_t}^{p_b}\beta dp} = \frac{1}{b}\left[\frac{\gamma}{\displaystyle\int_{p_t}^{p_b}\gamma dp} - \frac{(1 - b)Q_2}{\displaystyle\int_{p_t}^{p_b}Q_2 dp}\right] \tag{24b}$$

$$\gamma = -\bar{\omega}\frac{\partial\bar{q}}{\partial p}. \tag{24c}$$

It is to be noted that in both the ultimate Kuo and Molinari's scheme, Q_1 and Q_2 must be known a priori. This is a shortcoming as in nature they vary in time.

h. Computational procedure

In the beginning, Eqs. (1) and (2) were used to check whether there was a net convergence of moisture in a conditionally unstable atmosphere. If the two conditions are satisfied then the parameterization was acti-

TABLE 3. Regression coefficients obtained by using different datasets of MONEX.

Dataset	Dependent variables	a_1	b_1	c_1	a_2	b_2	c_2
16–25 May 1979	δ_{950}, $\bar{\omega}$	0.839×10^6	0.141×10^4	9.594	0.743×10^6	-0.915×10^3	6.831
3–12 June 1979	δ_{950}, $\bar{\omega}$	0.387×10^4	0.133×10^3	0.482	0.144×10^5	-0.467×10^2	1.096
14–23 July 1979	δ_{900}, $\bar{\omega}$	0.104×10^7	0.183×10^5	17.57	0.229×10^5	-0.167×10^2	1.572

vated. The potential temperature θ_c and specific humidity q_c inside the clouds were calculated from a moist adiabat by an iterative procedure (Molinari, 1982). The moisture supply Q_q and Q_θ were then calculated from (5b) and (5c). Subsequently, the coefficients a_θ and a_q were calculated for each scheme using (12)–(20). These coefficients were substituted in (8) and (9) to calculate the apparent heat source $(Q_1)_K$ and moisture sink $(Q_2)_K$ for different versions of Kuo's scheme. The values thus obtained for each scheme were compared with observed estimates from (10) and (11). The rainfall rates for different schemes were then computed from (4) after substituting the corresponding values of a_θ and a_q for each scheme.

3. Datasets for the study

During MONEX-79, three special sets of observations were taken at intervals of 6 hours by ships that were stationed in the form of polygons over the Arabian Sea and the Bay of Bengal. Figure 1 shows the positions of the polygons during three different periods of MONEX-79. In each set, the 6 hourly (00, 06, 12 and 18 UTC) upper air observations for a period of 10 days were used. The first set comprises data from 16 to 25 May 1979. This represents the preonset phase of the monsoon. In the second set, the data from 3 to 12 June 1979 was used. This was the onset phase of the summer monsoon. The third set was from 14 to 23 July 1979 which represented a "break" in the monsoon. The above classifications were based on synoptic situations and satellite cloud pictures. In 1979 the onset of the monsoon was on 13 June over southwest peninsular India. As the monsoon advances from the southwest over the Arabian sea, its arrival over the second polygon in the Arabian Sea would precede the onset over land by a few days. Satellite pictures reproduced by Krishnamurti et al. (1979, 1980) show well organized cloud clusters over the polygon during 3–12 June 1979. This period thus represents an onset phase of the monsoon. A "break" in the monsoon was observed over north India from 14 to 25 July; this was followed by a revival on 26 July. Stationary ships were located over the northern Bay of Bengal during this period. Consequently, 14–23 July represents a phase of lean rainfall or a "break" monsoon spell. The chronological weather summary of Sikka and Grossman (1980) may be referred to for more detailed discussions on the synoptic situations.

The datasets described above were processed for internal consistency. Erroneous data were rejected and recalculated by comparison with observations of other ships. Missing observations were replaced by fitting a linear regression equation in time and space. A cubic spline was used to interpolate some of the data at regular intervals of 50 mb from 1000 to 100 mb. The horizontal derivatives, such as, $\nabla \cdot \mathbf{V}$, $\nabla \times \mathbf{V}$, etc. were obtained from regression coefficients as described by Mohanty and Das (1986). Any remaining noise in the data would have thus been smoothed by the least square technique used in the estimation of above derivatives. The divergence was suitably adjusted (O'Brien, 1970) to make the vertically integrated divergence vanish. The vertical velocity was calculated by the kinematic method (Mohanty and Das, 1986).

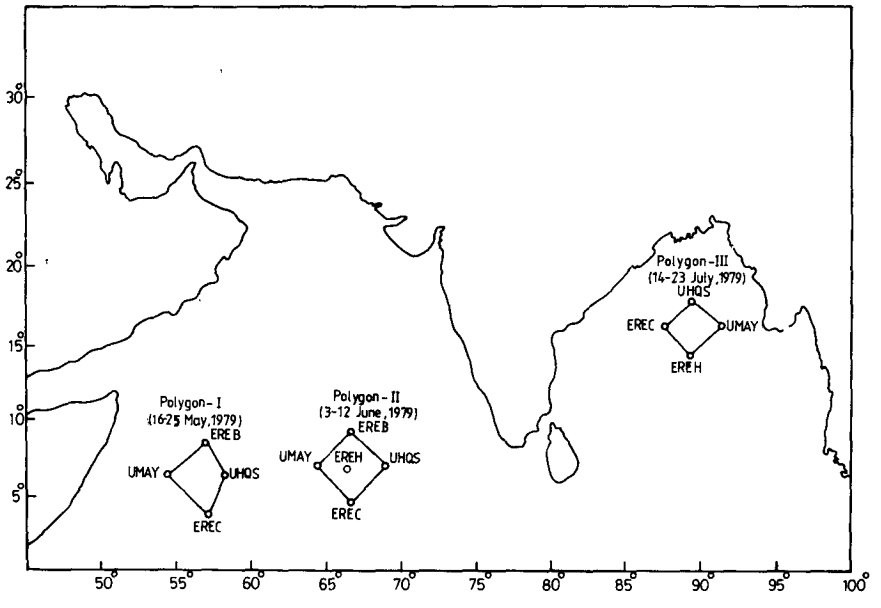

FIG. 1. Stationary positions of ships over the Arabian sea and the Bay of Bengal during MONEX-79.

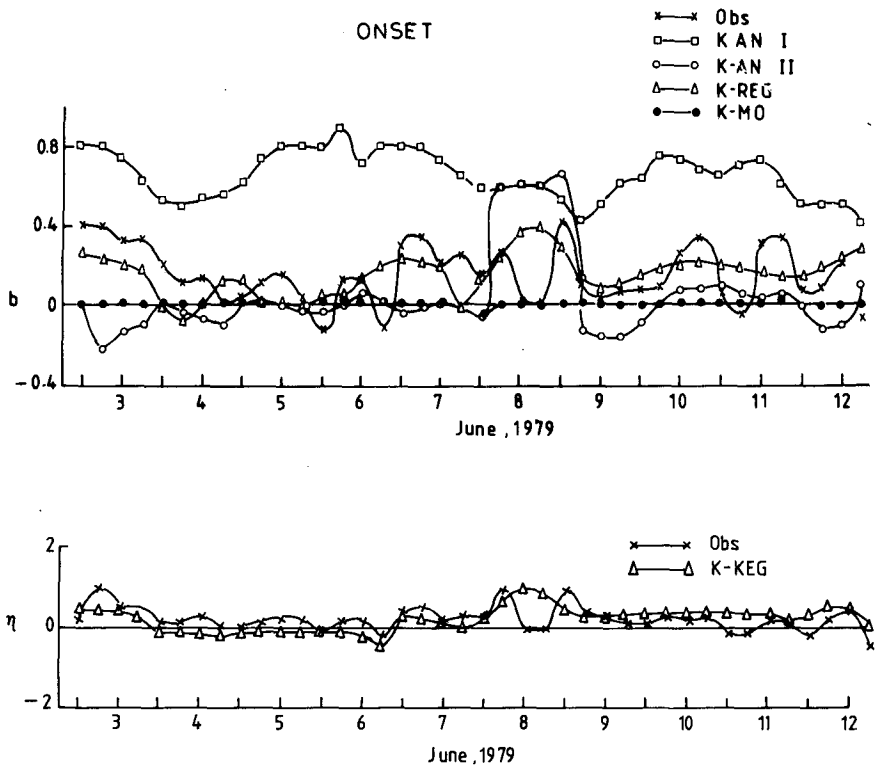

FIG. 2. Time series of (a) moistening parameter and (b) mesoscale convergence parameter obtained by different methods during the onset phase of the monsoon.

4. Results

The performances of different versions of Kuo's scheme were examined with three datasets corresponding to the preonset, onset and break phases of the summer monsoon. Results are, however, described in more detail for the onset period, because in this period organized large-scale deep convection was the main feature.

Figures 2a and 2b show the time series of the moistening parameter b and mesoscale convergence parameter 'η' during the onset phase. Table 4 shows the averaged values of b and η obtained by different methods during the three periods. The values of b in Fig. 2a were diagnostically calculated using (21a) and (21b). The figures show that, b and η calculated by different methods differ from each other. The values also vary in time. The smallest values of the moistening parameter were obtained by the method of Molinari (1982), while, the largest values were obtained by the method of Anthes (1977) with $n = 1$ and $RH_c = 0.5$. But, as it will be shown later, with this choice of parameters, the scheme gave very disappointing results. In an effort to minimize the errors, different combinations of n and RH_c were used to calculate heating, moistening and precipitation rates. An optimum value of $n = 5$ and $RH_c = 0$ was observed to provide the minimum errors during the three periods. This combination of n and RH_c also produced the minimum moistening parameter b in Molinari's (1982) scheme. The moistening parameter was negative on some occasions. This is difficult to interpret physically but, as noted by Cho (1976) and Fritsch et al. (1976), on such occasions the precipitation values exceeded the large-scale moisture supply. Variations of the mesoscale convergence parameter (η) with time show considerable fluctuations. The time series of b and η are not shown here for the other two periods, but, similar results were obtained during the other periods.

TABLE 4. Time averaged moistening parameter, b, and mesoscale convergence parameter, η, obtained by different Kuo type schemes during preonset, onset and break in the monsoon.

	Preonset		Onset		Break	
Method	b	η	b	η	b	η
K65	—	—	—	—	—	—
K74	0	—	0	—	0	—
K-AN I	0.95	—	0.68	—	0.54	—
K-AN II	0.025	—	0.006	—	0.002	—
K-REG	0.45	0.49	0.15	0.30	0.87	0.62
K-UL	0.19	0.06	0.15	0.25	−0.05	−0.36
K-MO	0.05	—	0.04	—	0.21	—

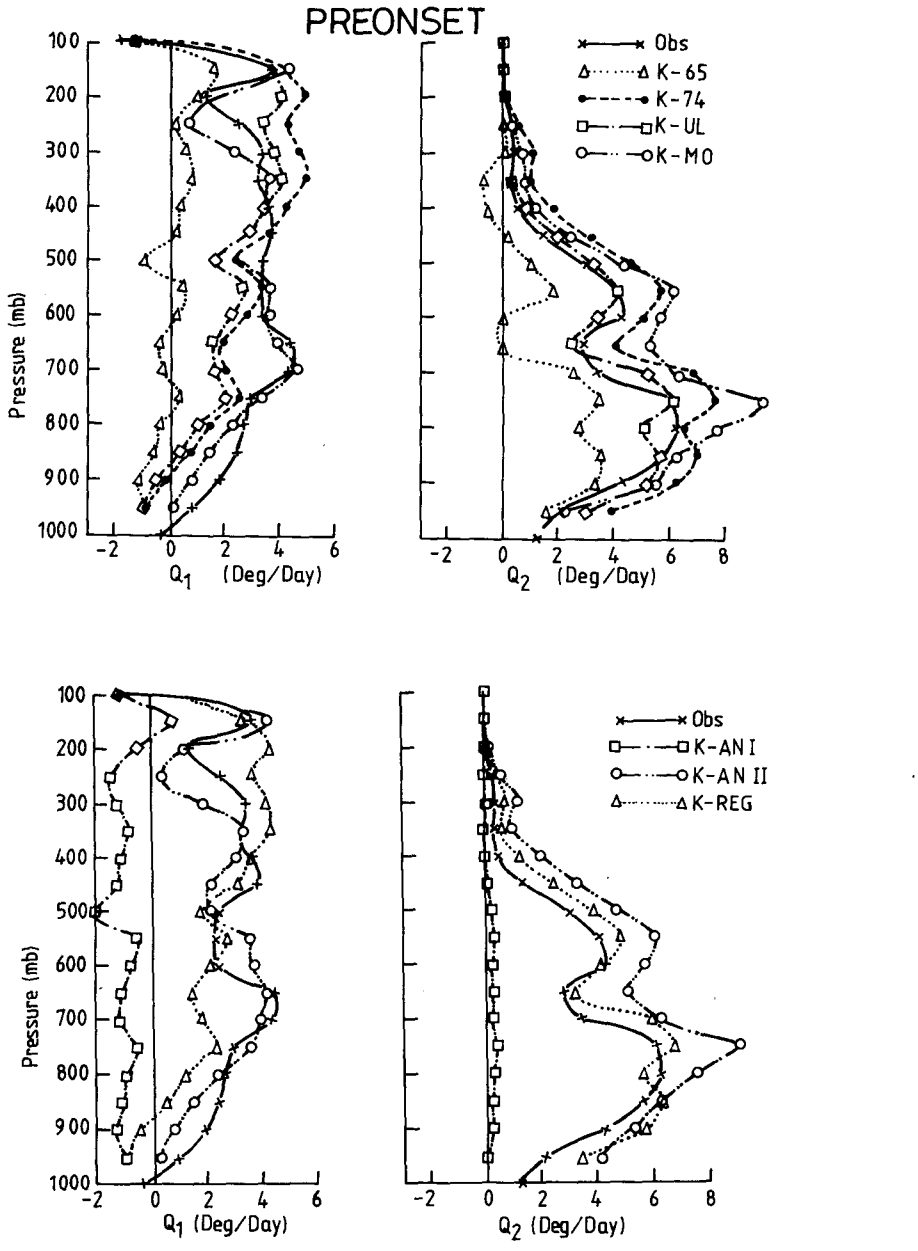

FIG. 3. Time averaged vertical profiles of observed apparent heat source Q_1, moisture sink Q_2 and those predicted by different types of Kuo scheme during the preonset period.

Figures 3–5 show the time averaged vertical profiles of the observed apparent heat source Q_1, moisture sink Q_2 and those simulated by the different versions of Kuo's scheme during the three phases of the summer monsoon. As we can see from these figures each scheme has a limitation in reproducing the observed profiles of Q_1 and Q_2. Schemes K65 and K-AN I produce the largest departures from observed profiles. The heating is underestimated at almost all levels by these two schemes. This is because these two schemes imply that most of the available moisture is stored in the atmosphere, and very little is condensed. The heating due to release of latent heat is consequently small. It was only after adjustment that the later scheme K-AN II provided results closer to observations. It is worth noting here that in a recent study by Mohanty et al. (1985), the modified Kuo-Anthes scheme with $n = 3$ and $RH_c = 0$ provided the best results with the ECMWF T63

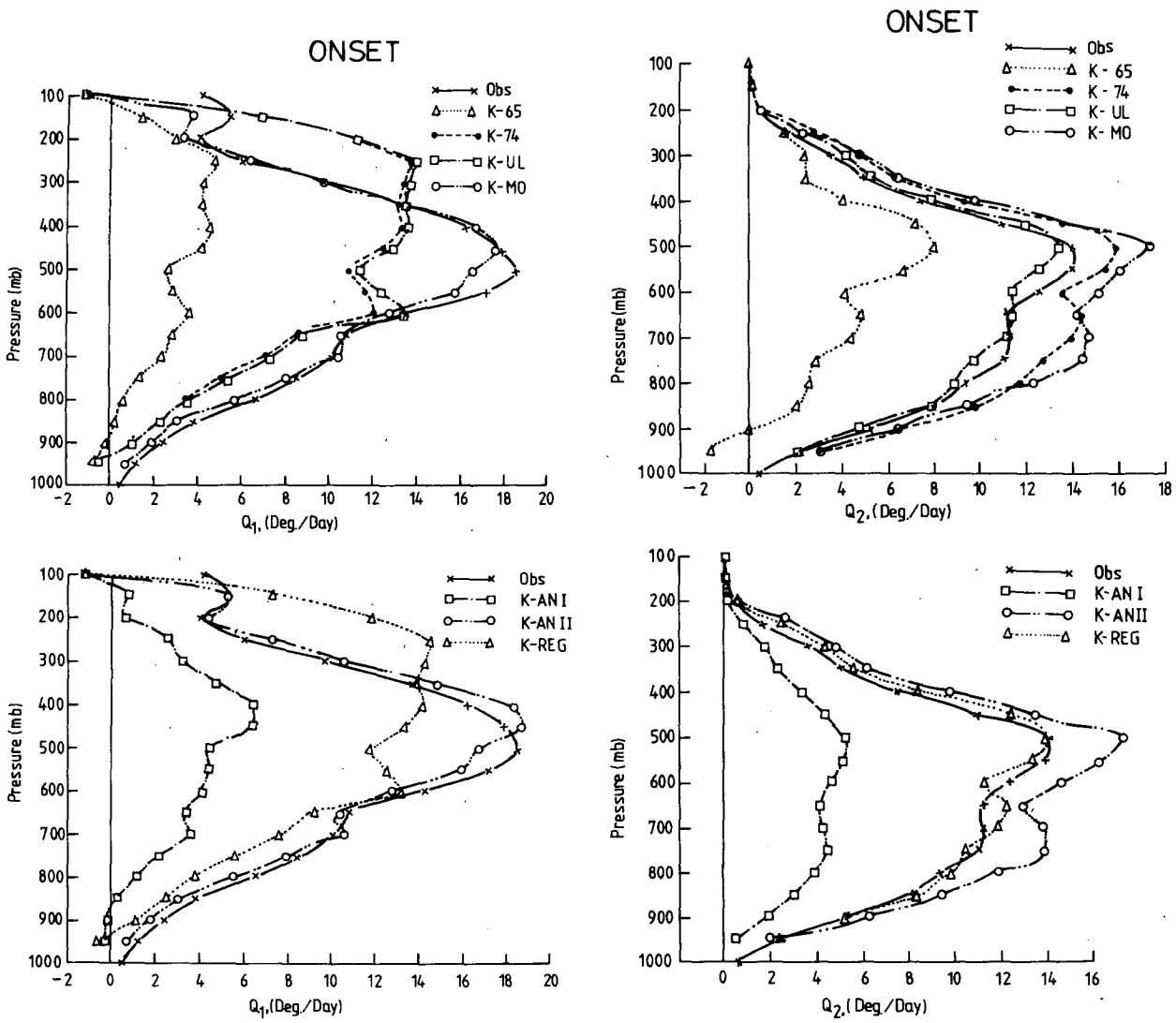

FIG. 4. As in Fig. 3 except for the onset period.

spectral model. Apparently, this combination of n and RH_c was tuned to the GATE dataset. In a study by Kuo and Anthes (1984), it was found that the best results were obtained with the Anthes scheme in a middle latitude convective system when n was between 2 and 3 and RH_c between 0.25 and 0.5. In the present study with three different synoptic situations of the summer monsoon, as well as in a case study during the formation of the monsoon depression with MONSOON-77 data (not discussed here), the minimum root-mean-square (rms) errors were obtained when n was between 3 and 5 and RH_c was between 0 and 0.25. Thus, the present investigation confirms the results of other studies on this aspect (Mohanty et al., 1985; Kuo and Anthes, 1984). A decrease in the value of RH_c and an increase in the value of n makes the moistening parameter 'b' smaller. Physically it means that a small moistening parameter is more appropriate in the present situations.

The profiles obtained by K74, K-UL and K-REG show considerable improvement in simulating the heating rates at lower levels up to about 600 mb. But these schemes fail to simulate the maximum heating rates observed at 500 mb. Above 400 mb in Fig. 3a and above 250 mb in Fig. 4a, the three schemes overestimate the heating rates. It is worth noting that the heating rates computed by the regression approach with the coefficients obtained by KLP from GATE data differed considerably from those obtained by using the coefficients calculated from MONEX data. The latter showed an obvious improvement because the regression coefficients for these cases were derived from their

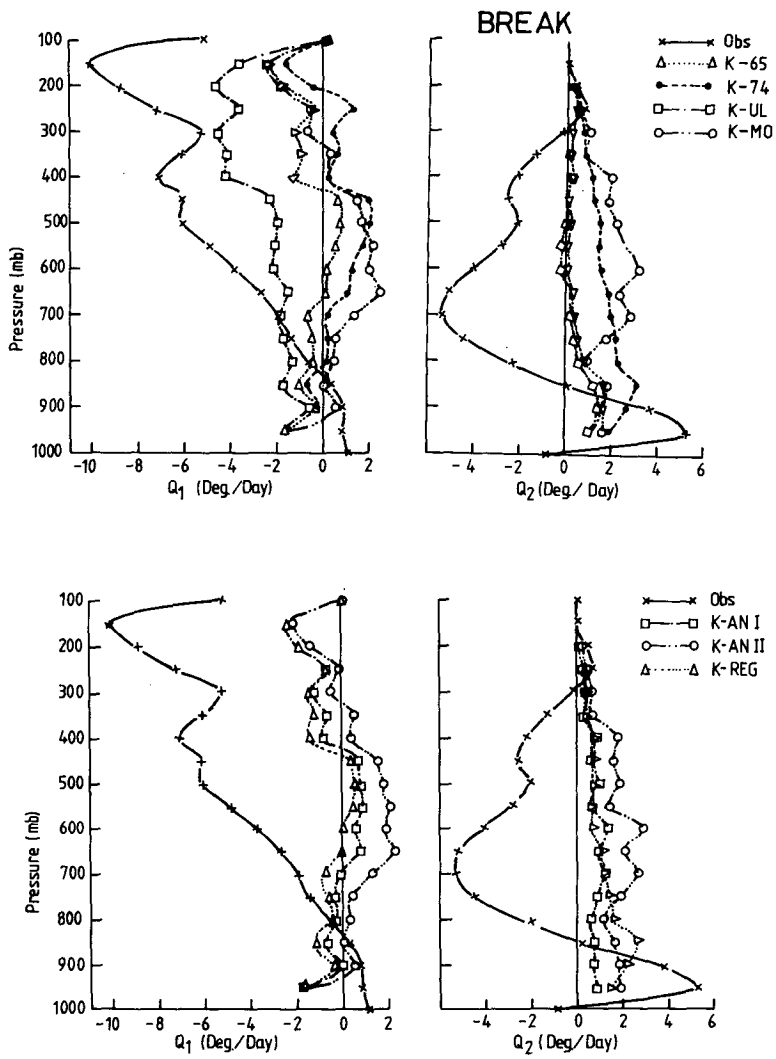

FIG. 5. As in Fig. 3 except for the break in monsoon.

respective datasets. The study showed that the regression approach did not provide encouraging results when coefficients derived from data of one period were used to predict heating and moistening rates for another period. In a further study, the regression coefficients were calculated by combining the datasets of all 3 periods. Then by using these coefficients, the heating and moistening were calculated separately for each period. However, we found no encouraging results even by this approach. Compared to all the methods discussed above, the K-MO and K-AN II schemes showed considerable success in simulating the heating rates throughout the troposphere. The maximum heating rates observed at 500 mb during the onset period was also well simulated by these methods. However, these schemes did not show superiority in simulating the drying rates, where K-UL and K-REG provided relatively better profiles. Table 5 shows the rms error of heating, moistening and precipitation rates obtained by different methods during the three periods. The results discussed above are clearly reflected from this table.

Comparison of the results during the three periods shows that relatively better simulations of the heating and drying are obtained during the preonset period. The schemes K-AN II and K-MO showed relatively better performance over the remaining schemes during the preonset and onset phases. However, none of the schemes was able to simulate accurately the cooling and moistening rates observed during the break in monsoon. Incidentally, K65 and K-AN I have shown relatively better success in this period. But, the reduction in heating produced by these schemes was largely a consequence of reduced condensation and increased

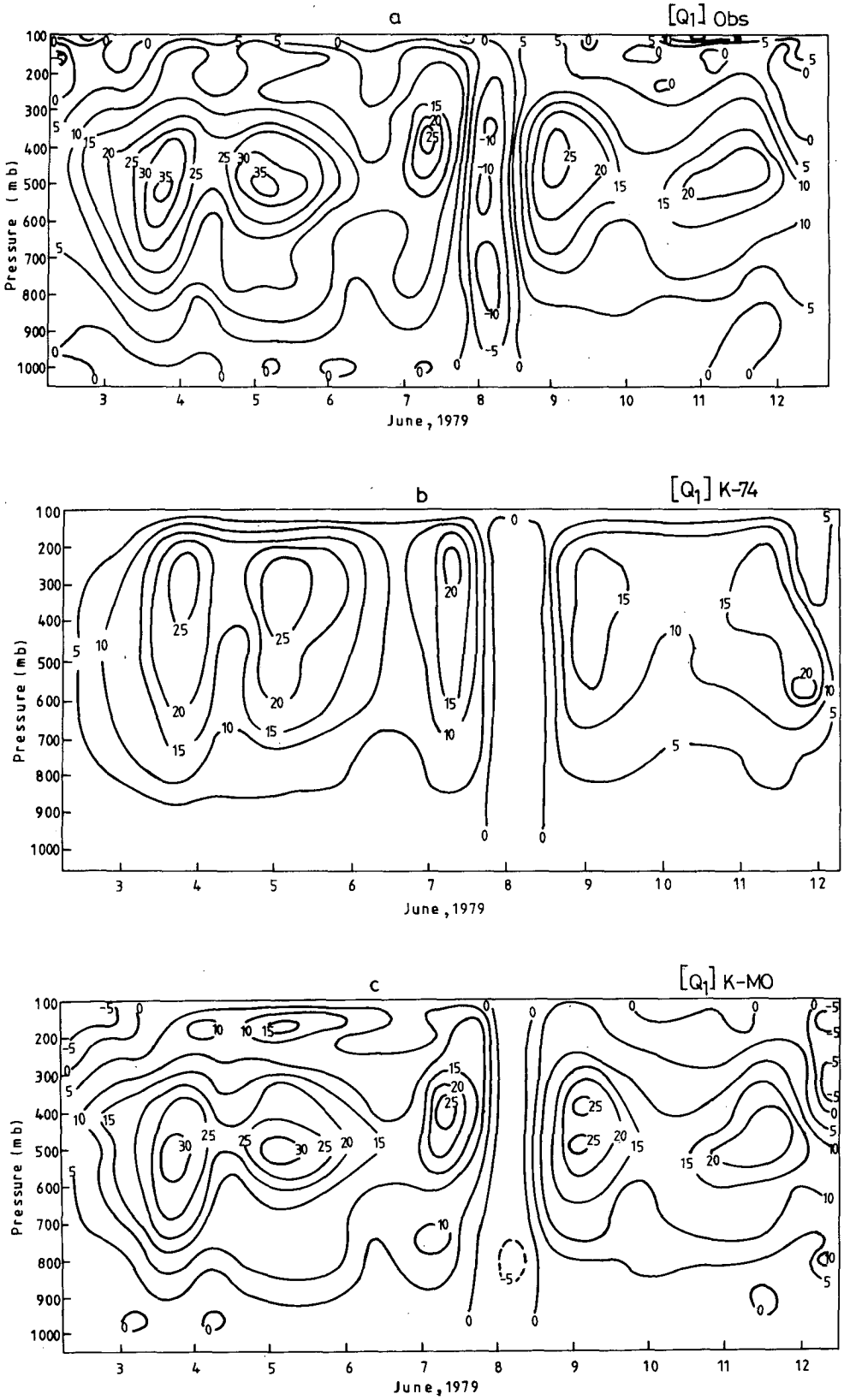

FIG. 6. Vertical time section of apparent heat source Q_1 (a) observed (b) simulated by K74 (c) simulated by K-MO and (d) simulated by K-AN II.

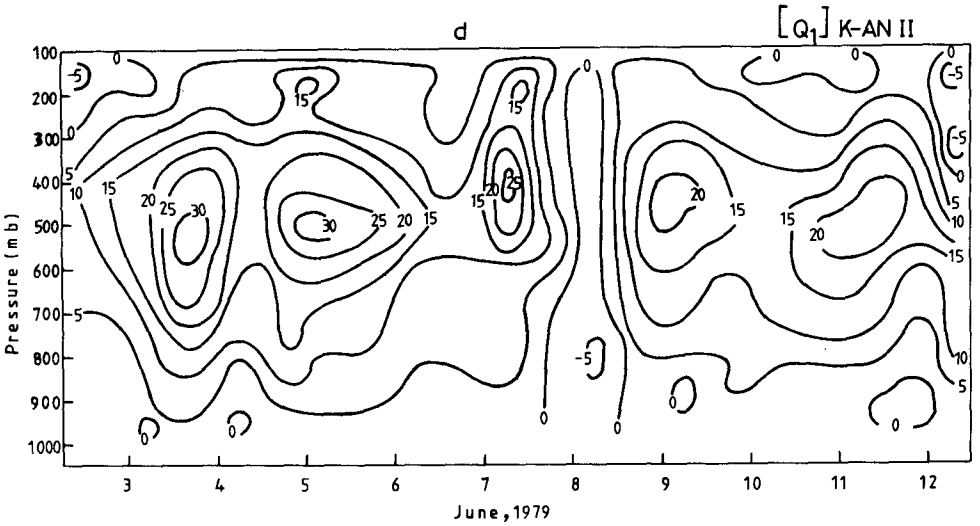

FIG. 6. (*Continued*)

moistening of the atmosphere. On the other hand, the cooling observed in this period is a combined effect of radiative heat loss and cooling produced by the evaporation of moisture in a relatively dry atmosphere.

Figure 6a–d show the vertical time sections of observed apparent heat source, and those simulated by K74, K-AN II and K-MO approaches during the onset period. The vertical time sections obtained by other methods are not illustrated but those analysis showed similar features as discussed in their respective averaged profiles. Figure 6a shows continuous heating from 4 to 7 and 9 to 12 June with pockets of maxima located around 450–550 mb. The maximum observed heating rate was 38°C day^{-1} at 550 mb on 5 June. The figure shows a sharp change from heating to cooling on 8 June. The periods of maximum heating are usually associated with the passages of cloud cluster over the polygon (Krishnamurti et al., 1979; Sikka and Grossman, 1980). The continuous heating from 4 to 7 and 9 to 12 June separated by pockets of maxima is an indication of rapid build up and decay of clouds during this period. The cooling on 8 June coincided with the dissipation of an Arabian Sea anticyclone. As a result, the flow was chaotic on that day. The cooling and moistening on 8 June seems to be an indication of the formative period of new cells as the classical low-level monsoon flow gradually commenced intensification. Figure 6b–d show that the two schemes K-MO and K-AN II have been able to accurately simulate the time and level of maximum heating rates on 4, 5, 7, 9 and 12 June. The time series of K74 shows that the maximum heating level is almost always too high in the troposphere. This is also evident from Fig. 4a.

Figure 7a–d shows the vertical time sections of observed and predicted apparent moisture sinks during the onset period. The figures show that the time of maximum drying ($Q_2 > 0$) coincided with the time of maximum apparent heating. The maximum equivalent heating due to the moisture sink was found to be about 34.4°C day^{-1} at 1200 UTC 5 June. This coincides with the time of maximum apparent heating. The level of maximum Q_2 was approximately the same as that of the Q_1 except on a few occasions when maximum Q_2 was located at a slightly lower level. Similar to the apparent cooling, a strong moistening ($Q_2 < 0$) occurred on 8 June. Figure 7b shows that the K74 scheme generally overestimated the drying rates, although the time and levels of maximum drying rates have been reproduced well. The excess drying rates simulated by this scheme are due to its choice of $b = 0$, which sets the moistening to zero. Its drastic consequence is seen on 8 June, when no moistening was reproduced by K74 scheme. On the other hand, K-MO and K-AN II have tried to produce a little moistening on 8 June. Although, K-MO has exaggerated the moistening rates observed on 3 June, the distribution of maximum drying rates has been fairly well simulated by both K-MO and K-AN II.

Figure 8a, b show the time series of precipitation rates measured by rain gauge, observed moisture budget (P_{Q_2}) and those simulated by various versions of the Kuo's scheme during the onset phase of the monsoon.

The figure shows that there is considerable difference between the rainfall measured by raingauges and those obtained by other methods. However, the precipitation simulated by different cumulus parameterization schemes show good agreement with that obtained from the observed moisture budget. The difference between measured rainfall rates and those obtained by other methods was also a feature of the other periods.

Discrepancies in the measurement of rainfall between ship board raingauges and the observed moisture

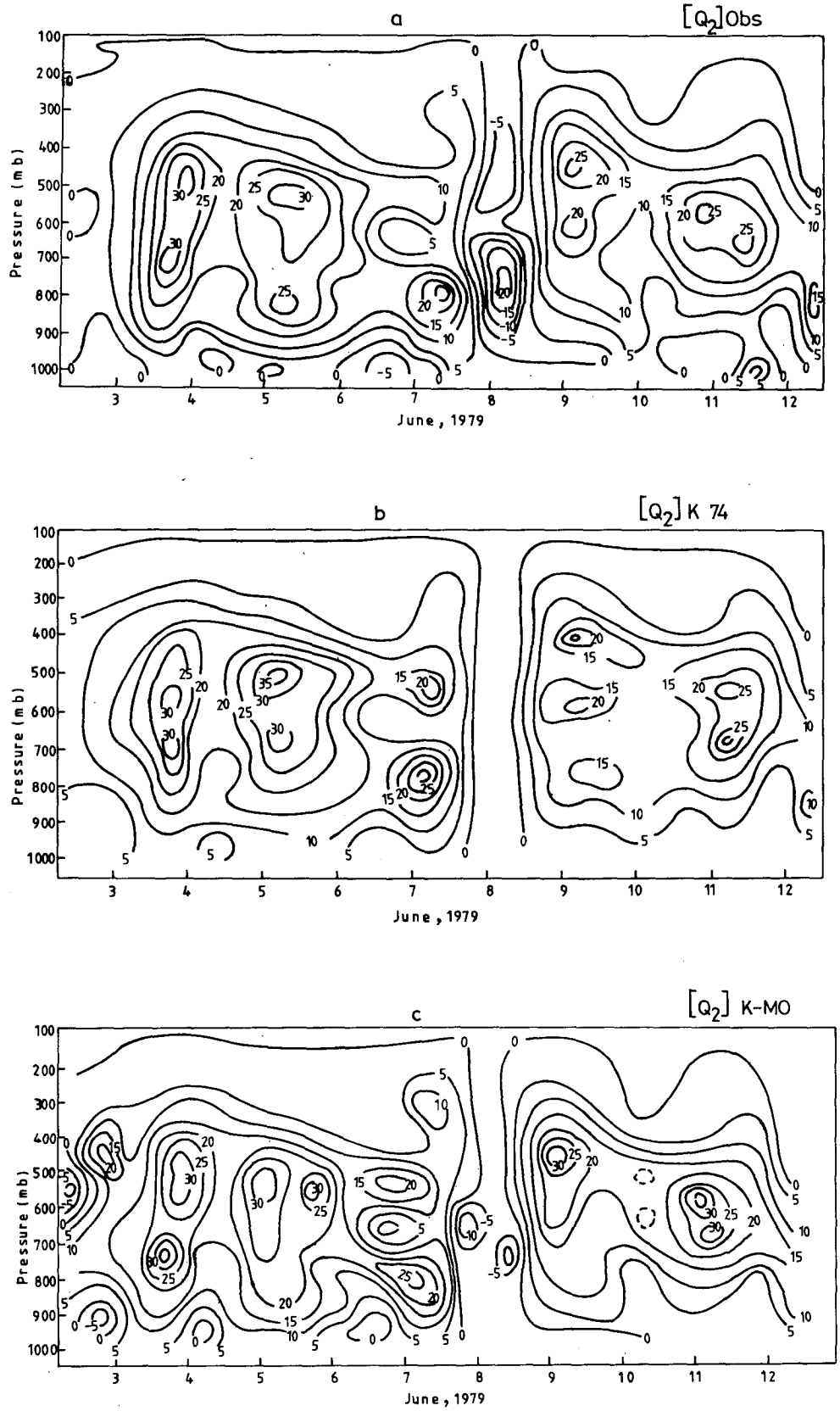

FIG. 7. As in Fig. 6 except for the apparent moisture sink Q_2.

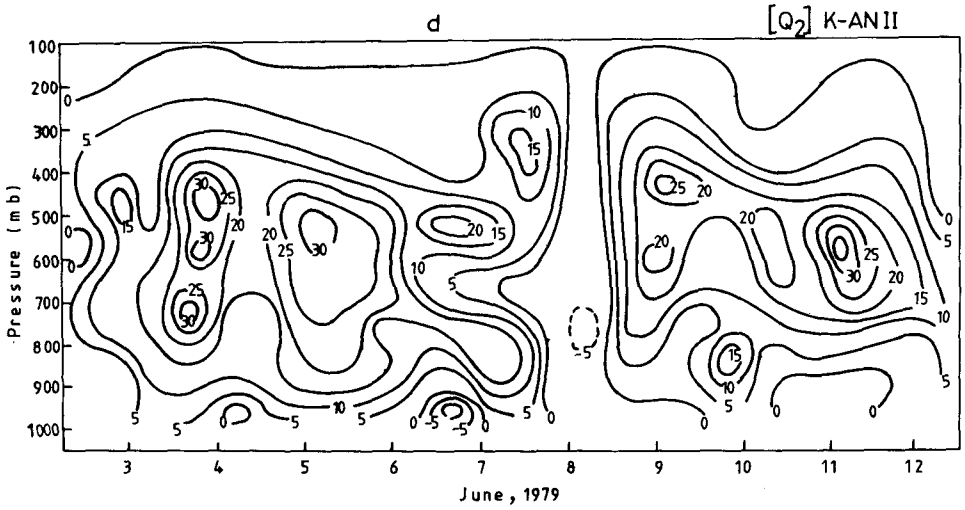

FIG. 7. (*Continued*)

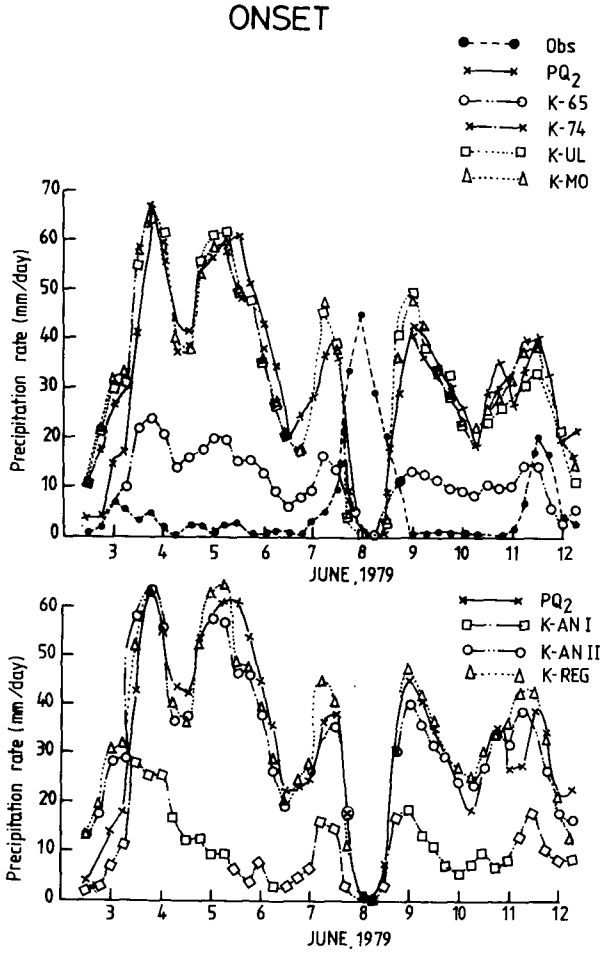

FIG. 8. Time series of precipitation rates obtained by rain gauge, observed moisture budget and those predicted by different types of Kuo schemes.

budget are most likely due to sampling error: four raingauges may not be able to represent the areal rainfall over the ship polygon adequately. Moreover, there were no measurements of rainfall by radar from the ships which would have been more reliable. The precipitation rates derived from satellite data by Krishnamurti et al. (1983a) (not reproduced here) also show much higher rainfall over the polygon area than those measured by shipboard raingauges, but nevertheless slightly less than that calculated here by different parameterization schemes. Table 6 shows the average rainfall rates obtained by different methods. The RMS errors of the rainfall rates simulated by different methods were given in the Table 5. It shows that, but for K65 and K-AN I, the RMSE of rainfall rates were approximately the same for the other methods. The rainfall rates obtained by the other 5 methods, i.e. K74, K-AN II, K-UL, K-REG and K-MO show good agreement with that obtained from observed moisture budgets. It is interesting to note that the maximum rainfall rates were usually preceded by a relative maximum in mesoscale convergence (Fig. 2b). The time lag was between 6 and 12 hours. The maximum rainfall rates also correspond to a relative minimum in the moisture storage of the atmosphere (Fig. 2a), with maximum heating and drying (Fig. 6a, 7a) of the troposphere. However, the correlation may not be considered as universal.

5. Discussion and conclusion

Different versions of the Kuo-type cumulus parameterization schemes have been studied during three different phases of the summer monsoon. The classical Kuo (1965) scheme underestimated cumulus heating, drying and rainfall rates. The moistening parameter

TABLE 5. Root-mean-square errors of cumulus warming, drying and precipitation rates obtained by various versions of the Kuo scheme during preonset, onset and break in the monsoon.

	Preonset			Onset			Break		
Method	Q_1 (°C day^{-1})	Q_2 (°C day^{-1})	Rainfall (mm day^{-1})	Q_1 (°C day^{-1})	Q_2 (°C day^{-1})	Rainfall (mm day^{-1})	Q_1 (°C day^{-1})	Q_2 (°C day^{-1})	Rainfall (mm day^{-1})
K65	2.9	1.7	16.7	8.2	4.9	26.1	4.7	2.9	10.8
K74	1.6	1.4	5.8	4.1	1.7	6.7	5.7	3.8	5.7
K-AN I	3.9	3.0	21.7	7.5	5.1	27.8	4.8	3.4	9.8
K-AN II	0.8	1.4	5.9	1.6	1.8	7.1	5.5	4.0	5.7
K-REG	1.6	1.0	16.7	4.0	0.7	6.1	4.6	3.4	12.5
K-UL	1.6	0.7	8.9	4.0	0.7	6.5	3.0	2.9	10.1
K-MO	0.8	1.4	7.0	1.5	2.1	7.0	5.4	4.1	5.9

computed by the method proposed by Anthes (1977) was high when $n = 1$ and $RH_c = 0.5$ were used. Consequently the heating, drying and rainfall rates were underestimated by this scheme as well. Optimum values of $n = 5$ and $RH_c = 0$ were found to provide the best results. The classical form of these two schemes provided relatively better simulation of the cooling and moistening during a break phase of the monsoon. Kuo (1974) provided considerable improvement in simulating the heating, drying and rainfall rates. But, the choice for this scheme of a very small moistening parameter (almost equal to zero) may cause unrealistic drying of the atmosphere in numerical weather prediction. This point has also been noted by many authors. Moreover, this scheme could not simulate the maximum heating at 500 mb observed during the onset period of the monsoon. The multiple regression approach and the ultimate Kuo scheme of Krishnamurti et al. (1983b) provides some improvement. A variable moistening parameter and mesoscale convergence parameter prove to be desirable features. Higher rainfall rates corresponded to a maximum heating and drying of the atmosphere. A limitation of the multiple regression approach was that the best results were obtained only when the regression coefficients were derived exclusively from the data to which the scheme was applied. This may produce a constraint on the regression approach for use in prognostic models. The limitation of the ultimate Kuo scheme has been noted by Krishnamurti et al. (1983b). The scheme can be used only for diagnostic purposes as it requires that Q_1 and Q_2 do not vary in time. The generalized Kuo scheme proposed by Molinari (1985) also improves the vertical distribution of heating and moistening but it suffers from the same shortcoming as the ultimate Kuo scheme. Considering these aspects, the adjusted Anthes scheme (K-AN II) seems to be preferable over the other schemes at present. Nevertheless it is also desirable to test this scheme in different monsoon years and at different locations.

TABLE 6. Time averaged rainfall rates obtained by various methods during preonset, onset and break in the monsoon.

Method	Preonset	Onset	Break
PQ_2	17.6	34.2	8.2
K65	4.3	10.9	1.8
K74	13.6	32.1	5.2
K-AN I	0.6	10.3	2.5
K-AN II	13.6	32.3	5.4
K-REG	12.2	34.3	1.4
K-UL	12.5	33.0	2.2
K-MO	13.7	32.8	5.1

An intercomparison of the results obtained during the three epochs of the monsoon show that the heating, moistening and precipitation rates are best simulated during a preonset period. This suggests that the present schemes work well when the convection is moderate.

Acknowledgments. We take this opportunity to express our gratitude to Prof. P. K. Das, I.I.T., Delhi for his useful comments on the original manuscript. The comments of the two anonymous referees are also acknowledged. They helped to improve the quality of the manuscript.

REFERENCES

Anthes, R. A., 1977: A cumulus parameterization scheme utilizing a one dimensional cloud model. *Mon. Wea. Rev.*, **105**, 270–286.

Cho, H. R., 1976: Effects of cumulus cloud activity on the large scale moisture distribution as observed on Reed-Recker's composite easterly waves. *J. Atmos. Sci.*, **33**, 1117–1119.

Fritsch, J. M., C. F. Chappell and L. R. Hoxit, 1976: The use of large-scale budgets for convective parameterization. *Mon. Wea. Rev.*, **104**, 1408–1418.

Krishnamurti, T. N., Y. Ramanathan, P. Ardanuy and R. Pasch, 1979: Quick Look "Summer MONEX Atlas" Part II, the onset phase. Rep. No. 79-5, Dept. of Meteorology, Florida State University, Tallahassee, Florida.

——, ——, ——, —— and P. Greiman, 1980: Quick Look "Summer MONEX Atlas" Part III, Monsoon depression phase, Rep. No. 80-8. Dept. of Meteorology, Florida State University, Tallahassee, Florida.

——, S. Cocke, R. Pasch and S. Low-Nam, 1983a: Precipitation estimates for raingauge and satellite observations. Rep. No. 83-7, Florida State University, Dept. of Meteorology, Tallahassee, Florida, 32306, pp. 1–373.

——, S. Low-Nam and R. Pasch, 1983b: Cumulus parameterization and rainfall rates II. *Mon. Wea. Rev.*, **111,** 815–828.

Kuo, H. L., 1965: On formation and intensification of tropical cyclones through latent heat release by cumulus convection. *J. Atmos. Sci.*, **22,** 40–63.

——, 1974: Further studies of the parameterization of the influence of cumulus convection on large scale flow. *J. Atmos. Sci.*, **31,** 1232–1240.

Kuo, Y.-H., and R. A. Anthes, 1984: Semiprognostic tests of Kuo-type cumulus parameterization schemes in an extratropical convective system. *Mon. Wea. Rev.*, **112,** 1498–1509.

Mohanty, U. C., J. M. Slingo and M. Tiedtke, 1985: Impact of modified physical processes on the tropical simulation in the ECMWF model. ECMWF Tech. Rep. 52, p. 45.

——, and S. Das, 1986: On the structure of the atmosphere during suppressed and active period of convection over the Bay of Bengal. *INSA J. Phys. Sci.*, **52**(A3), 625–640.

Molinari, J., 1982: A method for calculating the effects of deep cumulus convection in numerical models. *Mon. Wea. Rev.*, **110,** 1527–1534.

——, 1985: A general form of Kuo's cumulus parameterization. *Mon. Wea. Rev.*, **113,** 1411–1416.

O'Brien, J. J., 1970: Alternative solutions to the vertical velocity problem. *J. Appl. Meteor.*, **9,** 197–203.

Sikka, D. R., and B. Grossman, 1980: Summer MONEX chronological weather summary. Int. MONEX Management Centre, New Delhi.

Thompson, R., S. Payne, E. Recker and R. J. Reed, 1979: Structure and properties of synoptic-scale wave disturbances in the intertropical convergence zone in the eastern Atlantic. *J. Atmos. Sci.*, **36,** 53–72.